Path following algorithm and experiments for an incomplete symmetry unmanned amphibious platform

Yulong HUA, Wei SUN, Baoshan CHI, Guoqiang LIU
Department of Mechanical Engineering
Academy of Armored Forces Engineering
Fengtai, Beijing, 100072
People's Republic of China

Abstract: - The path following problem of incomplete symmetry unmanned amphibious platform was addressed. Considering the environmental disturbances the mathematical model of unmanned amphibious platform was established, and its control inputs were transformed from force and torque to water gate openings and pedal position. The path following error system, which was obtained after the former model being described in Serret-Frenet coordinate, was separated into two cascade subsystems, i.e., the position following subsystem and the orientation & surge velocity following subsystem. Then the equivalence between the second subsystem and the path following error system was proved on the basis of cascade theory. The globally asymptotically stable controller of orientation & surge velocity following subsystem was established based on backstepping adaptive sliding mode control method. The mathematic simulations and experimental tests were carried out, which illustrated that it was available for the incomplete symmetry unmanned amphibious platform to track the straight-line and circle path robustness under disturbances.

Key-words: - incomplete symmetry; unmanned amphibious platform; path following; Serret-Frenet frame; cascade theory; backstepping adaptive sliding mode control;

1 Introduction

Unmanned amphibious platform is a kind of intelligent equipment that emerges in recent years [1]. It can not only move relying on wheels or tracks, but also sail in the water by means of screw or propeller, which shows great military potential [2]. However, the platform is sensitive to environmental disturbances such as wind, wave and flow, and shows great nonlinearity, uncertainty, and time delay, which makes it difficult to follow a specified path [3]. There is a wide body of literature on developing controllers to solve this problem [4], [5], [6]. Path following methods for under- actuated vehicles in the presence of modeling uncertainty based on Lyapunov techniques are discussed in [7] and [8]. By introducing a virtual controlled degree of freedom for the target to be followed, Bibuli proposed a nonlinear Lyapunov- based control law in [9], which successfully yields a USV converge to the origin, and similar methods can be found in literature [10], [11]. In [12], J. Ghommam proposed a change of coordinates that transforms the whole system into a cascade nonlinear system, and a time-invariant discontinuous feedback law is derived to guarantee global uniform asymptotic stabilization of the system. In [13], Encarnacao considered a fourth order ship model subjected to constant direction ocean current disturbance in the Serret-Frenet frame, and developed a control strategy to follow both the straight line and the circle. YU Rui-ting proposed a new decoupling method of a non-symmetric surface vessel in [14]. The vessel's dynamic system was decoupled into two linear sub- systems based on

global diffeomorphism and time varying coordinate transformation, and got a global k-exponential stabilizing controller. Based on the cascade approach, GAO Jian proposed a globally k-exponentially stable path following controller of an underactuated autonomous surface vehicle in [15]. In the aforementioned papers, the mass and damping matrices of the vehicles are assumed to be diagonal, which does not hold for the unmanned amphibious platform completely. The platform shows great asymmetry because of the rotation of turret or the variation of loads, etc. In this paper, we proposed a controller to steer an incomplete symmetry unmanned amphibious platform along a predefined path at the presence of environmental disturbances induced by wave, wind, and current.

2 Problem Formulation

The kinematic and dynamic model of the incomplete symmetry unmanned amphibious platform can be described as [16].

$$
\begin{cases}
\dot{x} = u\cos\psi - v\sin\psi \\
\dot{y} = u\sin\psi + v\cos\psi \\
\dot{\psi} = r
\end{cases}
\tag{1}
$$

$$
\begin{cases}
m_{11}\dot{u} - m_{22}vr - \dfrac{m_{23}+m_{32}}{2}r^2 + d_{11}u = X + X_w \\
m_{22}\dot{v} + m_{23}\dot{r} + m_{11}ur + d_{22}v + d_{23}r = 0 \\
m_{32}\dot{v} + m_{33}\dot{r} - (m_{11}-m_{22})uv + d_{32}v \\
\quad + d_{33}r + \dfrac{m_{23}+m_{32}}{2}ur = N + N_w
\end{cases}
\tag{2}
$$

where x, y and ψ denote the surge displacement, sway displacement and yaw angle in the earth fixed frame; u, v and r denote surge, sway, and yaw velocities respectively. The positive constant terms m_{11}, m_{22}, m_{33}, m_{23} and m_{32} denote the platform inertia including added mass. The positive terms d_{11}, d_{22}, d_{33}, d_{23} and d_{32} represent the hydrodynamic dampings, and $d_{11}= n_u u^{w-1}$, where n_u and w denote damping and curve fitting coefficients respectively. The bounded time varying terms, X_w and N_w, are the force and moment induced by environmental disturbances such as wave, wind, and current with $|X_w| \leq X_{wmax} < \infty$

and $|N_w| \leq N_{wmax} < \infty$. The available control is the thruster force X and yaw moment N. As the sway control force is not available in the sway dynamics, the platform's model is underactuated [17].

Our objective is to design the surge force X and yaw moment N to force the underactuated platform Eqs. (1) and (2) to follow a specified path $\boldsymbol{\Omega}$, as is shown in Fig. 4, where P is a reference point to be followed by the platform. If we are able to drive the platform to follow P closely, then the control objective is fulfilled. Build a right-hand orthogonal coordinate system originated at point P, i.e., Serret-Frenet system [18,19], with the axes x_{sf} and y_{sf} oriented along the tangent and normal directions respectively, and ψ_p is the angle between x and x_{sf}. Let the location of the platform barycenter O in Serret-Frenet system ({SF} for short) be (τ_e, n_e), and $\psi_e = \psi - \psi_p$, then τ_e, n_e and ψ_e form a new set of state coordinates for platform. It can be seen that when the path $\boldsymbol{\Omega}$ coincides with the x axis, the above variables coincide with the ship variables x, y and ψ.
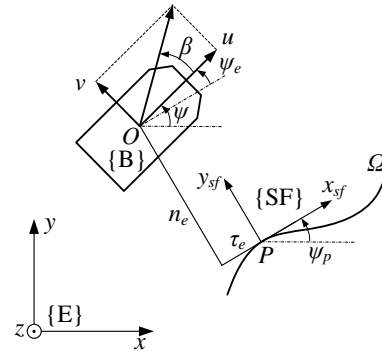

Fig. 1 General framework of platform path following

Let the coordinate of P be $(x_p(\omega), y_p(\omega))$, where ω is the path parameter variable. Hence, the velocity of point P moving along $\boldsymbol{\Omega}$ is

$$
U_P = \dot{\omega}\sqrt{\dot{x}_P^2 + \dot{y}_P^2}
\tag{4}
$$

The angle and yaw velocity is

$$
\psi_P(\omega) = \arctan\frac{\dot{y}_P(\omega)}{\dot{x}_P(\omega)}
\tag{5}
$$

$$
r_P(\omega) = \frac{\partial\psi_P}{\partial\omega}\dot{\omega} = \frac{\dot{x}_P(\omega)\ddot{y}_P(\omega) - \dot{y}_P(\omega)\ddot{x}_P(\omega)}{\dot{x}_P^2(\omega) + \dot{y}_P^2(\omega)}\dot{\omega}
$$

By applying the above parameterization, it is rather straightforward to transform the kinematics of

Eq. (1) to

$$\begin{cases} \dot{\tau}_e = -U_P + r_P n_e + u\cos\psi_e - v\sin\psi_e \\ \dot{n}_e = -r_P \tau_e + u\sin\psi_e + v\cos\psi_e \\ \dot{\psi}_e = r - r_P \end{cases} \qquad (6)$$

With Eq.(6), the control objective can be formally stated as follows: design the surge force X and the yaw moment N, to make the incomplete symmetry platform Eqs. (1) and (2) follow the predefined path Ω given by $(x_P(\omega), y_P(\omega))$, at the desired surge velocity $u_d(t)$.

Define the surge velocity following error as

$$u_e = u - u_d \qquad (7)$$

Define the drift angle as

$$\beta_d = \arctan\frac{v}{u_d} \qquad (8)$$

Substituting Eqs. (7) and (8) into Eq. (6) yields

$$\begin{cases} \dot{\tau}_e = -U_P + r_P n_e + U_d\cos\phi + u_e\cos\psi_e \\ \dot{n}_e = -r_P \tau_e + U_d\sin\phi + u_e\sin\psi_e \\ \dot{\phi} = \dot{\psi}_e + \dot{\beta}_d \end{cases} \qquad (9)$$

where the reference total velocity is $U_d = \sqrt{u_d^2 + v^2}$ and $\phi = \psi - \psi_P + \beta_d$.

Define the desired angle as

$$\phi_d = -\arctan\left(k_n n_e\right), \phi_d \in \left(-\frac{\pi}{2}, \frac{\pi}{2}\right) \qquad (10)$$

where $k_n > 0$ is a positive constant to be selected later.

Then the angle following error is

$$\phi_e = \phi - \phi_d \qquad (11)$$

Hence, the corresponding angular velocities are

$$\Omega = \dot{\phi} = r - r_P + \dot{\beta}_d$$
$$\Omega_e = \dot{\phi}_e = \Omega - \dot{\phi}_d = r - r_P + \dot{\beta}_d - \dot{\phi}_d$$

Substituting Eq. (11) into Eq. (9) yields two interconnected systems in cascade form [20]:

$$\begin{bmatrix} \dot{\tau}_e \\ \dot{n}_e \end{bmatrix} = \begin{bmatrix} -U_P + r_P n_e + U_d\cos\phi_d \\ -r_P \tau_e + U_d\sin\phi_d \end{bmatrix}$$

$$+ \begin{bmatrix} U_d\dfrac{\cos\phi - \cos\phi_d}{\phi_e} & 0 & \cos\psi_e \\ U_d\dfrac{\sin\phi - \sin\phi_d}{\phi_e} & 0 & \sin\psi_e \end{bmatrix} \begin{bmatrix} \phi_e \\ \Omega_e \\ u_e \end{bmatrix} \qquad (12a)$$

$$\begin{bmatrix} \dot{\phi}_e \\ \dot{\Omega}_e \\ \dot{u}_e \end{bmatrix} = \begin{bmatrix} \Omega_e \\ \dot{r} - \dot{r}_P + \ddot{\beta}_d - \ddot{\phi}_d \\ \dot{u} - \dot{u}_d \end{bmatrix} \qquad (12b)$$

Lemma 1: Consider the following two cascade time-varying subsystems [21]:

$$\sum_1 : \dot{x}_1 = f_1(t, x_1) + G(t, x)x_2 \qquad (13a)$$

$$\sum_2 : \dot{x}_2 = f_2(t, x_2, u) \qquad (13b)$$

where $x = [x_1, x_2]^T$, $f_1(t, x_1)$ is a continuously differentiable function of (t, x_1), $f_2(t, x_2, u)$ and $G(t, x)$ are both continuous and locally Lipschitz functions [22].

If the following assumptions are all satisfied, then the cascade system Eq. (13) is uniformly globally asymptotically stable.

(1) Subsystem $\dot{x}_1 = f_1(t, x_1)$ is uniformly globally exponentially stable;

(2) Subsystem $\sum_2$ is asymptotically stable;

(3) There were two continuous functions θ_1: $R^+ \rightarrow R$ and θ_2: $R^+ \rightarrow R$ that make $G(t, x)$ satisfy: $\|G(t, x)\|_2 \le \theta_1(\|x_2\|_2) + \theta_2(\|x_2\|_2)\|x_1\|_2$, where $\|\cdot\|_2$ denotes the 2-norm of vector or matrix [23].

We now state the Theorem 1 whose proof is given later on the basis of Lemma 1.

Theorem 1: If there exists a control law that renders the system (12b) globally asymptotically stable, then the cascade system consists of Eqs. (12a) and (12b) is also uniformly globally asymptotically stable under the control law.

Proof: Theorem 1 can be proved in 3 steps.

Define $x = [x_1, x_2]^T$, $x_1 = [\tau_e, n_e]^T$, $x_2 = [\phi_e, \Omega_e, u_e]^T$,

$$G(t, x) = \begin{bmatrix} U_d\dfrac{\cos\phi - \cos\phi_d}{\phi_e} & 0 & \cos\psi_e \\ U_d\dfrac{\sin\phi - \sin\phi_d}{\phi_e} & 0 & \sin\psi_e \end{bmatrix}.$$

Step 1: While $x_2=0$, we can get

$$\dot{x}_1 = f_1(t, x_1) = \begin{bmatrix} -U_P + r_P n_e + U_d \cos\phi_d \\ -r_P \tau_e + U_d \sin\phi_d \end{bmatrix} \quad (14)$$

Therefore, subsystem Eq. (12a) can be viewed as system Eq. (14) perturbed by the output of system Eq. (12b).

As to system Eq. (14), define Lyapunov function as

$$V = \frac{1}{2}\left(\tau_e^2 + n_e^2\right)$$

Differentiating V along Eq. (14) yields

$$\dot{V} = -\tau_e\left(U_P - U_d\right) + \tau_e U_d\left(\cos\phi_d - 1\right) + n_e U_d \sin\phi_d$$

Set the velocity of point P as

$$U_P = U_d + k_\tau \tau_e \quad (15)$$

where k_τ is a positive constant to be selected later.

Consider the definition of desired angle Eq. (10). Obviously,

$$\sin\phi_d = -\frac{k_n n_e}{\sqrt{1+\left(k_n n_e\right)^2}}, \quad \left|\cos\phi_d - 1\right| \leq \left|\sin\phi_d\right|,$$

$$1+\left(k_n n_e\right)^2 \geq \sqrt{1+\left(k_n n_e\right)^2} \quad (16)$$

Substituting Eqs. (15) and (16) into $\dot{V}$, yields

$$\dot{V} \leq -\left(k_\tau - \frac{U_d k_n}{2}\right)\tau_e^2 - \frac{U_d k_n}{2}\frac{n_e^2}{1+\left(k_n n_e\right)^2} - \frac{U_d k_n}{2}$$

$$\left(\left|\tau_e\right| - \frac{\left|n_e\right|}{\sqrt{1+\left(k_n n_e\right)^2}}\right)^2$$

It is obvious that if the constants k_τ and k_n are selected to satisfy the inequation

$$k_\tau > \frac{U_d k_n}{2} \quad (17)$$

then $\dot{V} \leq 0$, which implies the system Eq. (14) is globally uniformly asymptotically stable. The first assumption of Lemma 1 is satisfied.

Step 2: For convenience, the function $G(t, x)$ can be written as follows:

$$G(t, x) = G_1(t, x) + G_2(t, x)$$

$$= \begin{bmatrix} U_d \dfrac{\cos\phi_e \cos\phi_d}{\phi_e} & 0 & \cos\psi_e \\[2mm] U_d \dfrac{\sin\phi_e \cos\phi_d}{\phi_e} & 0 & \sin\psi_e \end{bmatrix} +$$

$$\begin{bmatrix} -U_d \dfrac{\sin\phi_e \sin\phi_d + \cos\phi_d}{\phi_e} & 0 & 0 \\[2mm] U_d \dfrac{\cos\phi_e \sin\phi_d - \sin\phi_d}{\phi_e} & 0 & 0 \end{bmatrix}$$

The result follows from the norm property:

$$\left\|G_1(t, x)\right\|_2^2 \leq \sum_{i=1}^{2}\sum_{j=1}^{3} g_{ij}^2 = U_d^2 \frac{\cos^2\phi_d}{\phi_e^2} + 1 \leq \frac{U_d^2}{\phi_e^2} + 1$$

Hence,

$$\left\|G_1(t, x)\right\|_2 \leq \sqrt{\frac{U_d^2}{\phi_e^2} + 1} = \theta_1\left(\left\|x_2\right\|_2\right).$$

Similarly,

$$\left\|G_2(t, x)\right\|_2 \leq \sqrt{\frac{U_d^2}{\phi_e^2}\left(\sin^2\phi_d + 2\sin\phi_d \sin\left(\phi_e - \phi_d\right) + 1\right)}$$

$$\leq \left|\frac{U_d}{\phi_e}\right|\left(\left|\sin\phi_d\right| + 1\right) = \left|\frac{U_d}{\phi_e}\right|\left(\frac{\left|k_n n_e\right|}{\sqrt{1+\left(k_n n_e\right)^2}} + 1\right)$$

$$= \theta_2\left(\left\|x_2\right\|_2\right)\left\|x_1\right\|_2$$

Therefore, it is obvious that

$$\left\|G(t, x)\right\|_2 \leq \left\|G_1(t, x)\right\|_2 + \left\|G_2(t, x)\right\|_2$$

$$\leq \theta_1\left(\left\|x_2\right\|_2\right) + \theta_2\left(\left\|x_2\right\|_2\right)\left\|x_1\right\|_2$$

The third assumption of Lemma 1 is satisfied.

Step 3: To satisfy the second assumption of Lemma 1, we thereafter need to design a discontinuous time varying control law that renders subsystem (12b) globally asymptotically stable.

3 Controller Design

It can be easily proven that the system Eq. (12b) does not satisfy Brockett's necessary condition and hence there's no continuous time-invariant state

feedback control law that renders the subsystem (12b) asymptotically stable about the origin [24, 25]. Therefore, a discontinuous time-varying control law is developed on the basis of backstepping technique and adaptive sliding mode control method, which is much more robust to the environmental disturbances.

Obviously, the third equation of Eq. (12b) is independent from the two former ones, hence, Eq. (12b) can be decomposed into two independent subsystems, i.e., the orientation error subsystem (18) and the surge velocity error subsystem (19).

$$\sum\nolimits_1 : \begin{cases} \dot{\phi}_e = \Omega_e \\ \dot{\Omega}_e = f_n + B_n N + B_n N_w \end{cases} \qquad (18)$$

$$\sum\nolimits_2 : \dot{u}_e = f_x + B_x X + B_x X_w \qquad (19)$$

where, $f_n = \dfrac{m_{22}(m_{11}-m_{22})}{M_h}uv - \dfrac{(m_{22}m_{23}-m_{11}m_{32})}{M_h}ur$

$-\dfrac{(m_{22}d_{32}-m_{32}d_{22})}{M_h}v - \dfrac{(m_{22}d_{33}-m_{32}d_{23})}{M_h}r - \dot{r}_P + \ddot{\beta}_d - \ddot{\phi}_d$,

$B_n = \dfrac{m_{22}}{M_h}$, $f_x = \dfrac{m_{23}r^2 + m_{22}vr - d_{11}u}{m_{11}} - \dot{u}_d$, $B_x = \dfrac{1}{m_{22}}$,

$M_h = m_{22}m_{33} - m_{23}m_{32}$.

3.1 Controller design for $\sum_1$

There are two steps to design the controller that stabilizes $\sum_1$.

Step 1: Design the sliding mode surfaces of the orientation error subsystem Eq. (18) as:

$$\begin{cases} z_1 = \phi_e \\ z_2 = \Omega_e - \theta_n(z_1) \end{cases} \qquad (20)$$

where $\theta_n(z_1)$ is a virtual stabilizing function to be selected later.

Step 2: By means of backstepping technique, define the Lyapunov function and prove the system's asymptotic stabilization.

Define the 1st Lyapunov function as $V_{11} = \phi_e^2 / 2$, and differentiating V_{11} along Eq. (20), yields

$$\dot{V}_{11} = z_1 \left[z_2 + \theta_n(z_1) \right] \qquad (21)$$

Let the virtual stabilizing function $\theta_n(z_1)$ be

$$\theta_n(z_1) = -k_{11}z_1 \qquad (22)$$

where k_{11} is a positive constant to be selected later.

Substituting Eq. (22) into Eq. (21), yields:

$$\dot{V}_{11} = -k_{11}z_1^2 + z_1z_2$$

Define the 2nd Lyapunov function as

$$V_{12} = V_{11} + \frac{1}{2}z_2^2 + \frac{1}{2\lambda_n}\tilde{N}_w^{\,2}$$

where $\tilde{N}_w = N_w - \hat{N}_w$, $\hat{N}_w$ is the estimation value of the torque N_w in yaw imposed by the environmental disturbances, $\tilde{N}_w$ is the estimation error of N_w, and λ_n is a positive constant to be selected later.

Substituting Eq. (18) into Eq. (20), yields

$$\begin{cases} \dot{\theta}_n(z_1) = k_{11}^2 z_1 - k_{11}z_2 \\ \dot{z}_2 = \dot{\Omega}_e - \dot{\theta}_n = f_n + B_n N + B_n N_w - \dot{\theta}_n \end{cases}$$

Differentiating V_{12} along Eq. (20) yields

$$\dot{V}_{12} = \dot{V}_{11} + z_2\dot{z}_2 + \frac{1}{\lambda_n}\tilde{N}_w\dot{\tilde{N}}_w$$

$$= -k_{11}z_1^2 + z_1z_2 + z_2\dot{z}_2 - \frac{1}{\lambda_n}\tilde{N}_w\dot{\hat{N}}_w$$

$$= -k_{11}z_1^2 - \frac{1}{\lambda_n}\tilde{N}_w(\dot{\hat{N}}_w - \lambda_n B_n z_2) + z_2(z_1 + f_n + B_n N$$

$$+ B_n\hat{N}_w - \dot{\theta}_n) \qquad (23)$$

In order to stabilize system Eq. (18), design the adaptive control law as

$$\begin{cases} N = -\left[z_1 + f_n + B_n\hat{N}_w - \dot{\theta}_n + k_{12}z_2 + \beta_n \,\mathrm{sgn}(z_2) \right] / B_n \\ \dot{\hat{N}}_w = \lambda_n B_n z_2 \end{cases} \qquad (24)$$

where sgn(x) is the sign function, k_{12} and β_n are positive constants to be selected later.

Substituting Eq. (24) into Eq. (23), yields

$$\dot{V}_{12} = -k_{11}z_1^2 - k_{12}z_2^2 - \beta_n |z_2| \le 0 \text{, therefore, subsystem}$$

Eq.(18) is asymptotically stable.

3.2 Controller design for $\sum_2$

Similarly, we can design the following adaptive control law to render the surge velocity subsystem Eq.(19) asymptotically stable about the origin.

$$\begin{cases} X = -\left[f_x + B_x \hat{X}_w - \dot{u}_d + k_x u_e + \beta_x \operatorname{sgn}(u_e) \right] \Big/ B_x \\ \dot{\hat{X}}_w = \lambda_x B_x u_e \end{cases} \quad (25)$$

where $\hat{X}_w$ is the estimation value of the force X_w in surge imposed by the environmental disturbances, λ_x, k_x, and β_x are positive constants to be selected later.

Based on the results above, a theorem is given as follows.

Theorem 2: The system Eq. (12b) is asymptotically stabilized by the adaptive control laws (24) and (25).

The proof is directly given from the above designing process. Consequently, under the corresponding control laws, the system (1) and (2) is asymptotically stabilized according to Theorem 1.

In order to eliminate the chattering and vibration, we use the saturation function to replace the sign function, i.e., sat(s) is used instead of sgn(s).

$$\operatorname{sat}(s) = \begin{cases} 1 & s > \Delta \\ ks & |s| \le \Delta \\ -1 & s < -\Delta \end{cases}$$

where Δ is the thickness of the boundary layer, k is a constant. In the paper, $\Delta = 0.5$, $k=1$.

4 Transformation of control inputs

The force X in surge and torque N in yaw of the unmanned amphibious platform are provided propellers, which are driven by the engine. It is much more realistic if we transform the control inputs from force and torque to the control variables of engine and propellers, i.e., pedal position and water gate openings respectively.

4.1 The transformation of water gate openings

As is shown in Fig. 2, two water jet propellers are located symmetrically on the platform at a distance $2l_1$. β_l and β_r denote left and right water gate opening, respectively. L and B denote the length and width of the platform, respectively. γ denotes the angle between the axis of the back off water tunnel and the surge direction; And l is the distance between point O and the tunnel portal along the surge direction. For simplicity, we assume that the relationship between the force and the water gate opening is linear. Hence, one has

$$\begin{cases} X_P = (1-t)T(\beta_r + \beta_l) - CT\cos\gamma\left[2 - (\beta_r + \beta_l)\right] \\ N_P = (l_1 + CL')T(\beta_r - \beta_l) \end{cases} \quad (26)$$

where $L' = l\sin\gamma + (B\cos\gamma)/2$, T denotes the force provided by one single propeller; C and t denote the reverse thrust factor and the thrust deduction fraction, respectively.
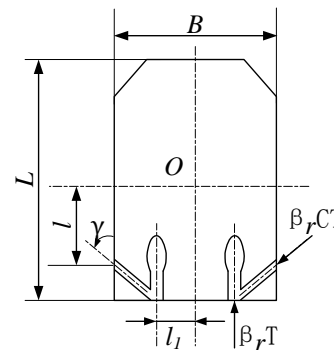

Fig. 2 The structure sketch of unmanned amphibious platform

In order to reduce the loss of surge velocity during change direction, let $X_P > 0$, then

$$\beta_r + \beta_l \ge \frac{2C\cos\gamma}{(1-t) + C\cos\gamma}$$

As to the unmanned amphibious platform we concerned, the parameters are as follows: $C = 0.8$, $t = 0.2$, $\gamma = 11.5°$. Therefore, we have

$$\beta_r + \beta_l \ge B_0 = 0.9899$$

Since the water gate openings are limited by mechanical structure, it is easy to know that $0 \le \beta_r, \beta_l \le 1$. Hence, the feasible region of water gate openings is about the shading area as shown in Fig.3.

In order to simplify the structure of control system and reduce the steering times, we choose the two bold lines as feasible region, as shown in Fig. 3.
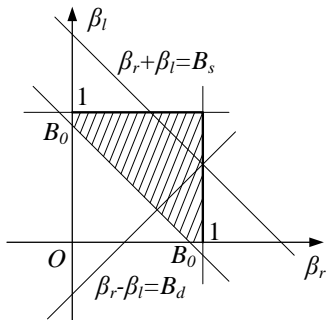

Fig. 3 The schematic diagram of propeller's water gates

4.2 The calculation of pedal position

According to [16], the thruster force T is determined by the engine, transmission, propellers, etc. The relationship among T, α and u is shown in Fig.4. If T and u is known, then α can be calculated by interpolation.
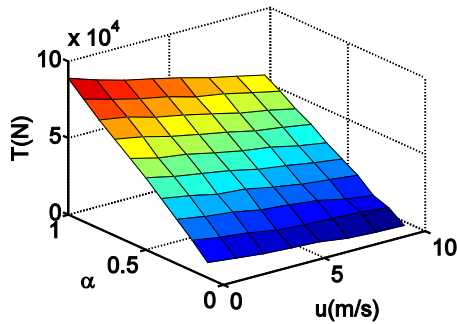
Fig.4 the curve among thruster force, surge velocity and pedal position

5 Numerical simulations

To verify the effectiveness of our controller, we present some simulations on an incomplete symmetry unmanned amphibious platform, whose parameters are given in Tab.1. And then the nominal parameters can be worked out according to [16]: m_{11} = 31727 kg, m_{22} = 32016 kg, m_{33}= 441570 kg·m^2, m_{23} = 3000 kg, m_{32} = 3000 kg, d_{11} = 447 kg/s, d_{22}= 14085 kg/s, d_{33} = 44747 kg·m^2, d_{23} = 4000 kg/s, d_{32} = 1600 kg/s.

Tab. 1 Parameters of unmanned amphibious platform

parameter	value	parameter	value
m/t	21.5	$draft/m$	1.04
$length/m$	9.2	n_u	65.86
$width/m$	3.2	W	3.11

In the simulation, the controller parameters are selected to be k_n=0.2, k_τ=1, k_{11} =10, k_{12} =0.2, k_x= 0.3, $\beta_x = 0.1$, $\beta_n = 0.1$, $\lambda_x = 1$, $\lambda_n = 1$.

The desired surge velocity u_d is set to be u_d =3m/s.

We assume that the environmental disturbances have the same order of magnitude as the thruster force, and then the disturbances can be defined as:

$$\begin{cases} X_w = -10000 + 5000\sin t + 5000\, rand(-1,1) \\ N_w = 5000\sin t + 5000\, rand(-1,1) \end{cases} \quad (27)$$
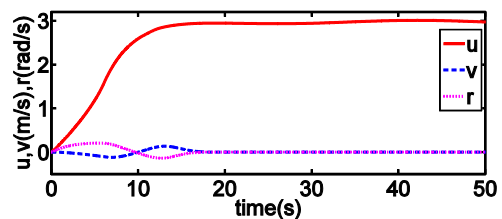
5.1 Straight line path following

The reference path is defined by Eq. (28), and the initial state values of the unmanned amphibious platform are set to be $x_0 = 10$ m, $y_0 = 0$ m, $\psi_0 = 0$ rad, $u_0 = 0$ m/s, $v_0 = 0$ m/s, $r_0 = 0$ rad/s. The simulation results are shown in Fig. 5.

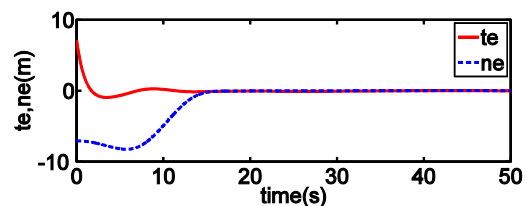$$\begin{cases} x = 10\omega \\ y = 10\omega \end{cases} \quad (28)$$

5.2 Circle path following

The circle path is defined as Eq. (29), and the initial state values are set to be x_0=0m, y_0=0m, ψ_0=0rad, u_0=0m/s, v_0=0m/s, r_0=0rad/s. The simulation results are shown in Fig. 6.
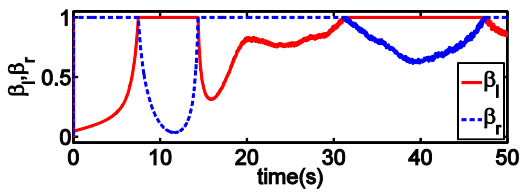
$$\begin{cases} x = 80\cos\omega \\ y = 80\sin\omega \end{cases} \quad (29)$$
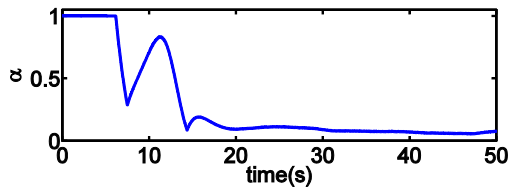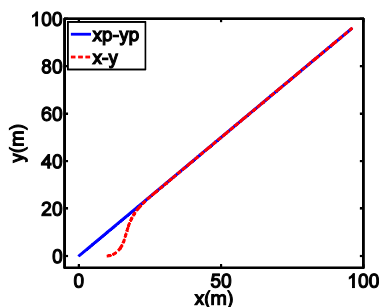

(a) The curve of platform's velocities

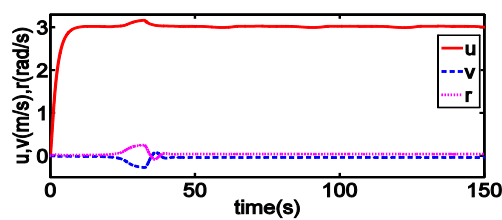(b) The curve of path following errors
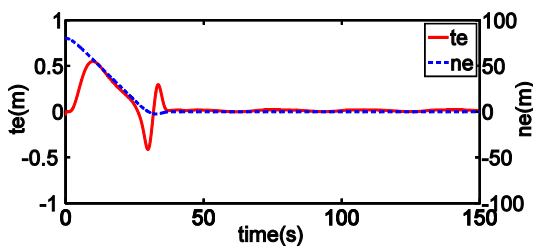
(c) The curves of water gate openings
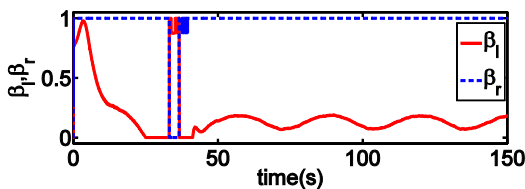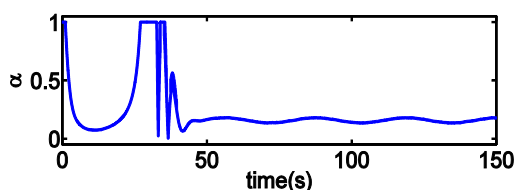

(d) The curve of pedal position

(e) The trajectory for straight-line path following
Fig. 5 Simulation results of straight-line path following

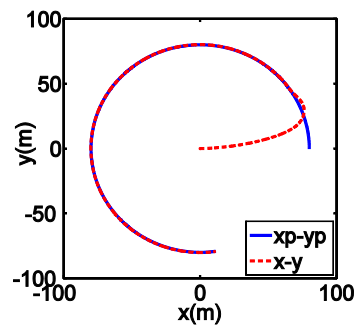(a) The curve of platform's velocities

(b) The curve of path following errors

(c) The curves of water gate openings

(d) The curve of pedal position

(e) The platform's trajectory for circle path following
Fig. 6 Simulation results of circle path following

Fig. 5 and Fig. 6 show that the proposed controller effectively completes the task of path following. The errors τ_e, n_e and u_e converge to zero quickly in spite of environmental disturbances. At the beginning of path following, the following errors are quite large. To reduce these errors immediately, the pedal is pushed to the end (100%), and the right water gate opening is up to maximum (100%) while the other side a little (4.5%). After the platform settles on the path, the pedal position and water gate openings should remain unchanged theoretically. But in reality, because of the presence of environmental disturbances, the control inputs vary in the same frequency with that of disturbances. Nevertheless, the following errors remain to be zero, which illustrates the robustness of our controller.

6 Experiment Analyses

6.1 Control system of unmanned amphibious platform

To further support out controller, we developed the control system of unmanned amphibious platform, as is shown in Figs. 7 and 8. The onboard controller is developed on the basis of TMS320F2812, which supports serial and Ethernet communications for digital and analog input/output. The pedal and water gates are operated by three DC motors (400 W, 48V), with a set of servo amplifiers. The navigation instrumentation set is constituted of a DGPS/INS and Mti-G-700 to compute position and the true north. Electrical power supply is provided by the onboard

generator. The Shore-based controller is developed based on a Yeston PT55D, with an operating system Linux running in it. The communications between shore-based controller and onboard controller is based on a pair of wireless modules.
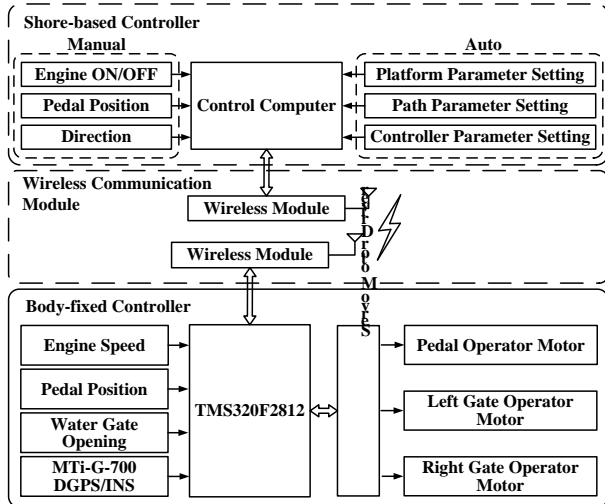

Fig. 7 Structural diagram of the platform's control system

Fig. 8 The shore-based controller

6.2 Experiment results and analyses

The straight line experimental tests were carried out at Chaohu Lake, Hefei, Anhui Province, the site is usually beaten by a 2 ~ 4m/s wind. The tests discussed in the following were performed in July, 2015, in calm wind conditions, and the initial state of the platform and controller parameters were the same as that of the simulations. The resulting performance of the controller is shown in Fig. 9.
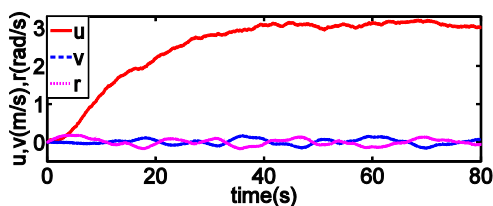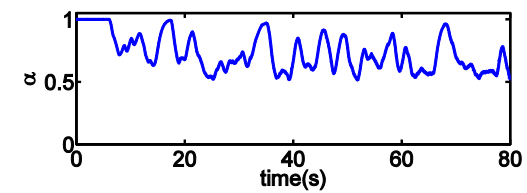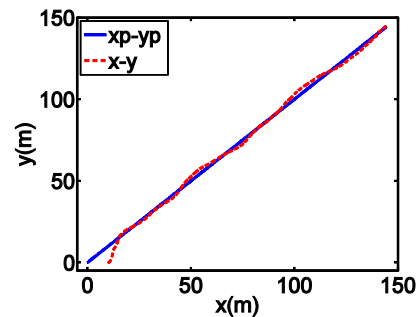

(a) The curve of platform's velocities
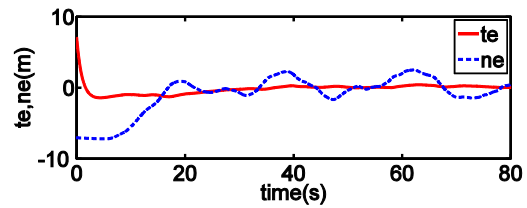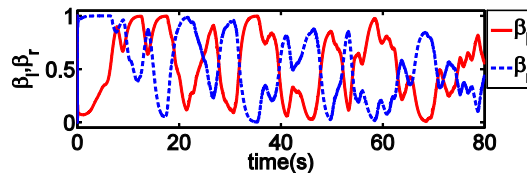
(b) The curve of path following errors

(c) The curves of water gate openings

(d) The curve of pedal position

(e) The platform's trajectory for circle path following
Fig. 9 Experimental results of straight line following

Compared with simulation, the experimental results basically hold that of the simulations in tendency. The surge velocity u and path following error T_e can fairly coincide that of simulations, while another path following error n_e oscillates along the origin, although the oscillating amplitude is under the tolerance. The oscillation is probably caused by the modeling errors or the perturbance of the water depth, which are not considered.

All in all, the experimental results are identical with that of simulations, and the controller manages to steer the in complete symmetry platform to track the straight-line and circle path.

7 Conclusions

In this paper, a framework has been presented for the problem of path following for an incomplete symmetry unmanned amphibious platform at the presence of environmental disturbances. A practical controller is designed on the basis of backstepping technique and adaptive sliding mode control method. Simulations show that the proposed controller accurately follows the straight-line and circle path despite the presence of environmental disturbances. Moreover, experimental tests are carried out to validate the effectiveness of the controller. The performances of experiment are identical with that of the simulations in terms of tendency. On the other hand, the experiment results perform badly in some aspects, such as the vibration of the following error, which may be caused by the unmodeled higher order disturbances or the asymmetries about the left-right axis. Absolutely these are the significant aspects to be studied in next work.

References:

[1] CHEN Hui-yan, ZHANG Yu. An overview of research on military unmanned ground vehicles [J]. *Acta Armamentarii*. 2014, 35(10): 1696 - 1706.

[2] LIU Fu-wei, XU Hai-tong, YANG Song-lin. Preliminary study on the rolling characteristics of an amphibious unmanned vehicle [J]. *Chinese Journal of Ship Research*, 2014, 9(1): 46 - 51.

[3] K. D. Do. Practical control of underactuated ships [J]. *Ocean Engineering*, 2010, 37(13): 1111 – 1119.

[4] Ashrafiuon Hashem, Muske, Kenneth R. Sliding mode tracking control of surface vessels [J]. *2008 American Control Conference* [C]. Seattle, United States: Institute of Electrical and Electronics Engineering Inc., 2008: 556-561.

[5] M. Breivik, V. E. Hovstein, T. I. Fossen. Straight-line target tracking for unmanned surface vehicles [J]. *Modeling, identification and control*. 2008, 29(4): 131 – 149.

[6] R. Skjetne, T. I. Fossen, P. V. Kokotovic. Robust output maneuvering for a class of nonlinear systems [J]. *Automatica*. 2014, 40(3): 373 – 383.

[7] A. Pedro Aguitar and Joao. P. Hespanha. Trajectory-tracking and path-follow- ing of underactuated autonomous vehicles with parametric modeling uncer- tainty [J]. *IEEE Transactions on automatic and control*. 2007, 52(8): 1362 – 1379.

[8] Yu-lei LIAO, Yu-min SU, Jian CAO. Trajectory planning and tracking control for underactuated unmanned surface vessels [J]. *Journal of Central South University of Technology*. 2014, 21(2): 540 - 549.

[9] Marco Bibuli, Gabriele Bruzzone, Massimo Caccia. Path-following algorithms and experiments for an unmanned surface vehicle [J]. *Journal of Field Robotics*. 2009: 26(8): 669 - 688.

[10] K. D. Do, Z. P. Jiang, J. Pan. Robust adaptive path following of underactuated ships [C]. *Proceedings of the IEEE conference on decision and control*. 2002, 3: 3243- 3248.

[11] K. D. Do, J. Pan. Global robust adaptive path following of underactuated ships [J]. *Automatica*. 2006, 42, (10): 1713 – 1722.

[12] J. Ghommam, F. Mnif, A. Benali, et al. Asymptotic backstepping stabilization of an underactuated surface vessel [J]. *IEEE transactions on control systems technology*. 2006, 14(6): 1150 - 1157.

[13] Encarnacao P, Pascoal A, Arcak M. Path following for autonomous marine craft[C]. *Proceedings of the 5th IFAC Conference on Maneuvering and Control of Marine Craft*. Alborg, Denmark: IFAC, 2000: 117 - 122.

[14] YU Rui-ting, ZHU Qi-dan, LIU Zhi-lin, et al. Decoupling implementation of global κ-expo- nential stabilization of underactuated non-symmetric vessel [J]. *Control and Decision*. 2012, 27(5): 781 - 786.

[15] GAO Jian, LIU Fu-qiang, ZHAO Jiang, et al. Non-linear path following control of under-actuated autonomous surface vehicles [J]. *Robot*. 2012, 34(3): 329 - 336.

[16] Ju Nai-jun. *Hydrodynamics Analysis and Simulation for Amphibious Vehicle* [M]. Beijing: Weapon Industry Press, 2005.

[17] Hitoshi Katayama, Hirotaka Aoki. Straight-line trajectory tracking control for sampled-data underactuated ships [J]. *IEEE Transactions on control systems technology*. 2014, 22(4): 1638 – 1645.

[18] HE Xiangyu, LIU Guixi. Improved Gaussian mixture PHD smoother for multi-target tracking [J]. *WSEAS Transactions on Signal Processing*. 2015, 11: 196-203.

[19] K. D. Do, J. Pan. Robust path following of underactuated ships using Serret-Frenet frame

[C]. *Proceedings of the 2003 American control conference*. 2003, 3: 2000 - 2005.

[20] MA Baoli. Global K-exponenitial asymptotic stabilization of underactuated surface vessels [J]. *Systems & control letters*. 2009, 58: 191 -201.

[21] LIAO Yu-lei, PANG Yong-jie, ZHANG Tie-dong. Global κ -exponential stabilization of underactuated autonomous surface vessels by a smooth time-varying feedback control [J]. *Journal of Harbin Engineering University*. 2011, 32(4): 417 - 422.

[22] E. Panteley, A. Loria. Growth rate conditions for uniform asymptotic stability of cascaded time-varying systems [J]. *Automatica*. 2001, 37: 453 - 460.

[23] Erjen Lefeber, Kristin Ytterstad Pettersen, et al. Tracking control of an underactuated ship [J]. *IEEE Transactions on control systems technology*. 2003, 11(1): 52 - 61.

[24] S. VASUHI, V. VAIDEHI. Target detection and tracking for video surveillance[J]. *WSEAS Transactions on Signal Processing*, 2014, 10: 168-177.

[25] F. Mazenc, K. Y. Pettersen, H. Nijmeijer. Global uniform asymptotic stabiliza- tion of an underactuated surface vessel [J]. *IEEE Transactions on automation and control*. 2002, 47(10): 1759 – 1762.